

Selective Voltammetric Determination of Nitrite Using Cobalt Phthalocyanine Modified on Multiwalled Carbon Nanotubes

To cite this article: Shun Lu et al 2020 J. Electrochem. Soc. 167 046515

View the <u>article online</u> for updates and enhancements.





Selective Voltammetric Determination of Nitrite Using Cobalt Phthalocyanine Modified on Multiwalled Carbon Nanotubes

Shun Lu, 1,*,Z Matthew Hummel, Shuai Kang, and Zhengrong Gu^{1,Z}

Nitrite (NO_2^-) is a ubiquitous inorganic pollutant presented in the food industry and drinking water. In addition, NO_2^- as a toxic contaminant probably threaten human health by producing N-nitrosamines with highly carcinogenic. Voltammetric biosensing is considered the most promising approach because it offers a fast, reliable, and low-cost detection. In this article, cobalt (II) phthalocyanine (CoPc) was immobilized on multiwalled carbon nanotubes (MWCNTs), then immobilized on glassy carbon electrode (GCE) as an electrochemical senor toward nitrite using the voltammetric technique. Consequently, differential pulse voltammogram (DPV) is employed for nitrite determination, which reached a linear dynamic range of 0.01 to 1050.0 mM with a detection limit (LOD) of 2.11 μ M. Such excellent performance is ascribed to the synergistic effect between CoPc and MWCNT, indicating the promise of applying CoPc/MWCNTs@GCE in the practical bio-sensing applications.

© 2020 The Electrochemical Society ("ECS"). Published on behalf of ECS by IOP Publishing Limited. [DOI: 10.1149/1945-7111/ab7982]

Manuscript submitted January 4, 2020; revised manuscript received February 8, 2020. Published March 4, 2020.

Supplementary material for this article is available online

Nitrite (NO $_2$) as a preservative is extensively used in the food industry, especially in the production and processing of pickled meat due to nitrite's ability to inhibit bacterial growth. ¹⁻⁴ Nitrite has become a ubiquitous inorganic pollutant presented in food, drinking water, soil, environment, and even physiological systems due to the colorless and odorless nature of nitrite. ^{3,5,6} It is reported that a level as low as 0.10 mg l $^{-1}$ of nitrite in freshwater is regarded as signs of toxicity. ⁷⁻⁹ Similarly, the European Union Scientific Committee for Food sets the acceptable daily intake (ADI) of NO $_2$ as 0.06 mg kg $^{-1}$ of body weight. ¹⁰ The U.S. Environmental Protection Agency has restricted the maximum contaminant level to 1.0 ppm (21.7 μ M), and a similar guideline value recommended by WHO is 3.0 ppm. ¹¹ Therefore, a fast, sensitive, and cost-effective method to detect nitrite in food and water is desired to ensure the protection of human health and the environment. ^{2,4,6,12,13}

Among the various techniques for nitrite sensing, electrochemical methods (i.e. differential pulse votammetry, cyclic voltammetry and amperometry) are regarded as favorable for quantitative analysis, owing to their fast response, high sensitivity, and ease-of-operation. ^{14–19} However, conventional electrodes (i.e. glassy carbon electrodes and screen-printed electrodes) possessing good conductivity, but low sensitivity and selectivity cannot satisfy the requirements of analyte detection at the same time. ¹⁷ To resolve this problem, various functional materials or micro-nano structures have been employed to enhance the detection response and sensitivity through a strategy of modification on the bare GCE. ^{2,20}

Metallophthalocyanines (MPcs) are employed in many fields owing to their high chemical and thermal stability, varied coordination properties, diverse substitutional alternatives, and potential electrochemical properties. This is especially true for cobalt (II) phthalocyanine (CoPc). ^{21–25} The electrocatalytic performance of CoPc is related to the Co(II)/Co(III) or Co(II)/Co(I) couples in these compounds. ²⁵ However, two main issues arise from using this material for nitrite detection: (a) CoPc usually peels off the glassy carbon as CoPc is physically adsorbed on the surface of the working electrode, (b) the conductivity of CoPc is poor, owing to its status as a semiconductor. ²⁶ The aforementioned drawbacks result in a general reduction of electroactivity and stability. Hence, choosing a proper supporting material as a host matrix which can enhance direct electron transfer rate between the electroactive species and

In this work, multiwalled carbon nanotubes (MWCNTs) were selected as host matrix, providing a suitable microenvironment for electroactive molecules and excellent support for CoPc. Here, CoPc and MWCNTs were purchased and pretreated with a simple method that the two chemicals were mixed with dimethylformamide (DMF) under ultrasonication, then centrifugation. As a result, a sensitive and stable electrochemical sensor based on CoPc/MWCNTs was fabricated and successfully achieved the determination of nitrite in phosphate-buffered solution.

Experimental

Materials.—Cobalt (II) phthalocyanine ($C_{32}H_{16}N_8C_0$, CoPc) and N,N-dimethylformamide (DMF) were purchased from Fisher Scientific, US. Multiwalled carbon nanotubes (MWCNTs) were brought from US Research Nanomaterials, Inc. Deionized water (DIW, 18.4 $M\Omega$) was prepared for all solutions in this study. Phosphate buffer solution (PBS, 0.1 M) consisting of NaH₂PO₄ and Na₂HPO₄ were also purchased from Fisher Scientific and was applied and then the pH value tuned with 0.1 M sodium hydroxide and phosphoric acid.

Preparation of CoPc/MWCNTs electrode.—Three steps to prepare CoPc/MWCNTs, as follows: (a) a mixture solution of CoPc (0.003 mmol, 2.0 mg dissolved in DMF), and MWCNTs (2.0 mg dissolved in DMF) was prepared, (b) ultrasonic agitation (30 min) and (c) centrifugation (washed with ethanol, 3 times), as illustrated in Fig. 1. Before modification, the bare glass carbon electrode (GCE, 4 mm in diameter) was polished with 0.01, 0.05, and 0.1 μ m Al₂O₃ and then washed ultrasonically in ethanol and DIW. Then, the working electrode was modified that 2 μ l of the CoPc/MWCNTs suspension (4 mg ml⁻¹, CoPc/MWCNTs dissolved in ethanol) was covered on the bare GCE and the solvent evaporated

¹Department of Agricultural and Biosystems Engineering, South Dakota State University, Brookings, South Dakota 57007, United States of America

²Chongqing Institute of Green and Intelligent Technology, Chinese Academy of Sciences, Chongqing, 400714, People's Republic of China

electrodes to improve the performance of nitrite sensor is desired. In addition, carbon-based materials (i.e. carbon nanotubes) are widely applied in the electrochemical detection owing to the excellent conductivity and high surface area since the discovery in 1991. Recently, Zhao et al. employed cobalt oxide decorated reduced graphene oxide and carbon nanotubes (Co₃O₄-rGO/CNTs) as a sensitive electrochemical nitrite sensor, in which Co₃O₄ played a key role in nitrite detection, and carbon-based materials (rGO and CNTs) usually having excellent conductivity, and provided more active sites to detect analytes which later produce stronger electrochemical signal responses.²⁷

^{*}Electrochemical Society Student Member.

^zE-mail: shun.lu@sdstate.edu; zhengrong.Gu@sdstate.edu

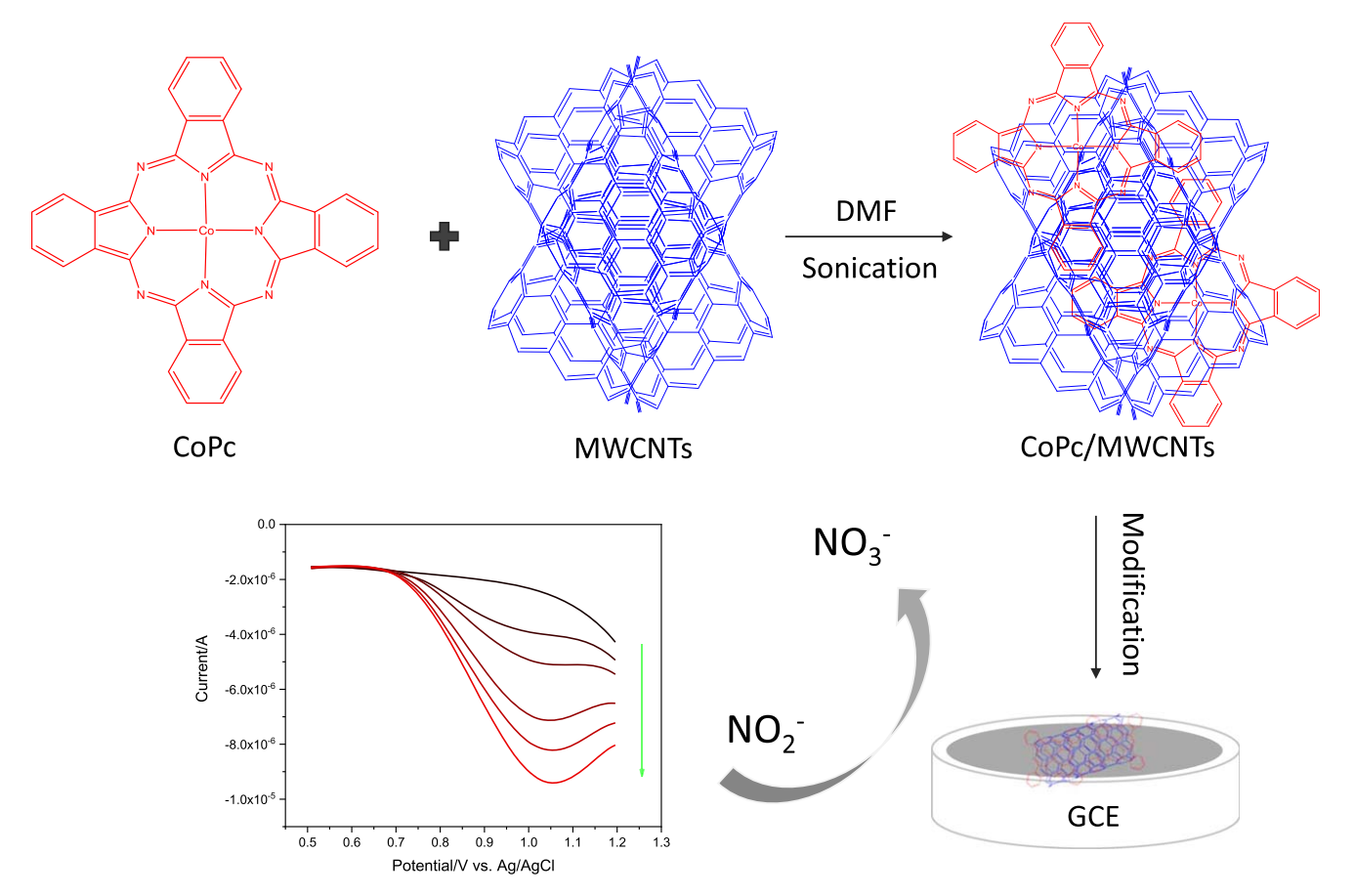


Figure 1. Schematic illustration for the preparation of CoPc/CNT composites and modification on GCE toward nitrite detection.

in air. CoPc and MWCNTs solution with same concentration were prepared for comparison.

Apparatus and measurements.—Morphological structure was observed employing a transmission electron microscope (TEM, JEM-2100, JEOL) equipped with scanning transmission electron microscope energy-dispersive X-ray spectroscopy (STEM-EDX, Gatan Inc.). Elemental mapping was used to analysis the elements content of the as-prepared composites under an acceleration voltage of 200 kV. All electrochemical measurements were carried out using an electrochemical workstation (CHI 760E, CH instruments. Inc., USA). A conventional configuration (three-electrode system) is employed, as follows, CoPc/MWCNTs modified GCE as a working electrode, platinum wire as counter electrode and an Ag/AgCl with saturated KCl solution as reference electrode.

Results and Discussion

Physical characterizations of the morphology of CoPc/MWCNTs.—The surface information of MWCNTs, CoPc and CoPc/MWCNTs were verified by using TEM. Figures 2a–2e show TEM images of the above samples with different magnifications. It can be clearly seen that MWCNTs are dispersed uniformly with a diameter of ∼18 nm (Fig. 2b), CoPc is composed of several nanosheets and those nanosheets are attached to each other (Figs. 2c–2d). MWCNTs are covered by CoPc, as shown in red dash line in Fig. 2e. In addition, it is obviously found that there is a transparent area in the center area (yellow dash line) of Fig. 2e. This area was also analyzed by STEM-EDX, as displayed in Figs. 2f–2k. Cobalt, carbon, and nitrogen elements were found (Fig. 2f). STEM-EDX mapping of the select area in Fig. 2e is in good agreement with the result of Fig. 2f. Combined with the TEM images and

STEM-EDX results, CoPc/MWCNTs are fabricated successfully using a simple method.

Electrocatalytic activity towards nitrite oxidation.—The electrocatalytic detection of CoPc/MWCNTs modified on GCE (CoPc/ MWCNTs@GCE) towards nitrite was studied. Figure 3a depicts the cyclic voltammograms (CVs) of CoPc@GCE, MWCNTs@GCE and CoPc/MWCNTs@GCE in 0.1 M PBS (pH 7.0). No apparent redox peak was appeared on these modified electrodes. However, it seemed that CoPc modified GCE (CoPc@GCE) shows the lowest value in comparison with MWCNTs and CoPc/MWCNTs modified electrodes' performance in terms of the electrochemical surface area (ESA), directly indicating the excellent conductivity of CNTs enhanced the CoPc/CNT nanocomposite's performance to some extent. As nitrite was introduced into the previous system, there is a stable oxidation peak appeared in each electrode, as shown in Fig. 3b. These phenomena indicated that nitrite suffered an irreversible redox process on those electrode surfaces. Furthermore, according to the previous report, the potential corresponded the oxidation peak for nitrite at the bare GCE was $\sim 1.12 \text{ V}$, however the potential at those modified electrodes shifted negatively to 0.972 V. The decrease in peak potential demonstrate that electroactivity towards nitrite on CoPc/MWCNT electrode was highly enhanced and keep consistent with the previous result (Fig. 3a), suggesting that the formation of CoPc/MWCNTs composites could promote the electroactivity owing to efficient electron transfer. 1,9,27,28 Herein, a simple selectivity test is carried out through differential pulse voltammograms (DPVs) with different nitrite concentration from 0 to 5 mM in 0.1 M PBS (pH 7.0). As displayed in Figs. 3c-3d, there are a series peaks around 1.0 V for CoPc modified electrode in Fig. 3c, it means nitrite oxidation occurred on the CoPc modified electrode. However, no obvious

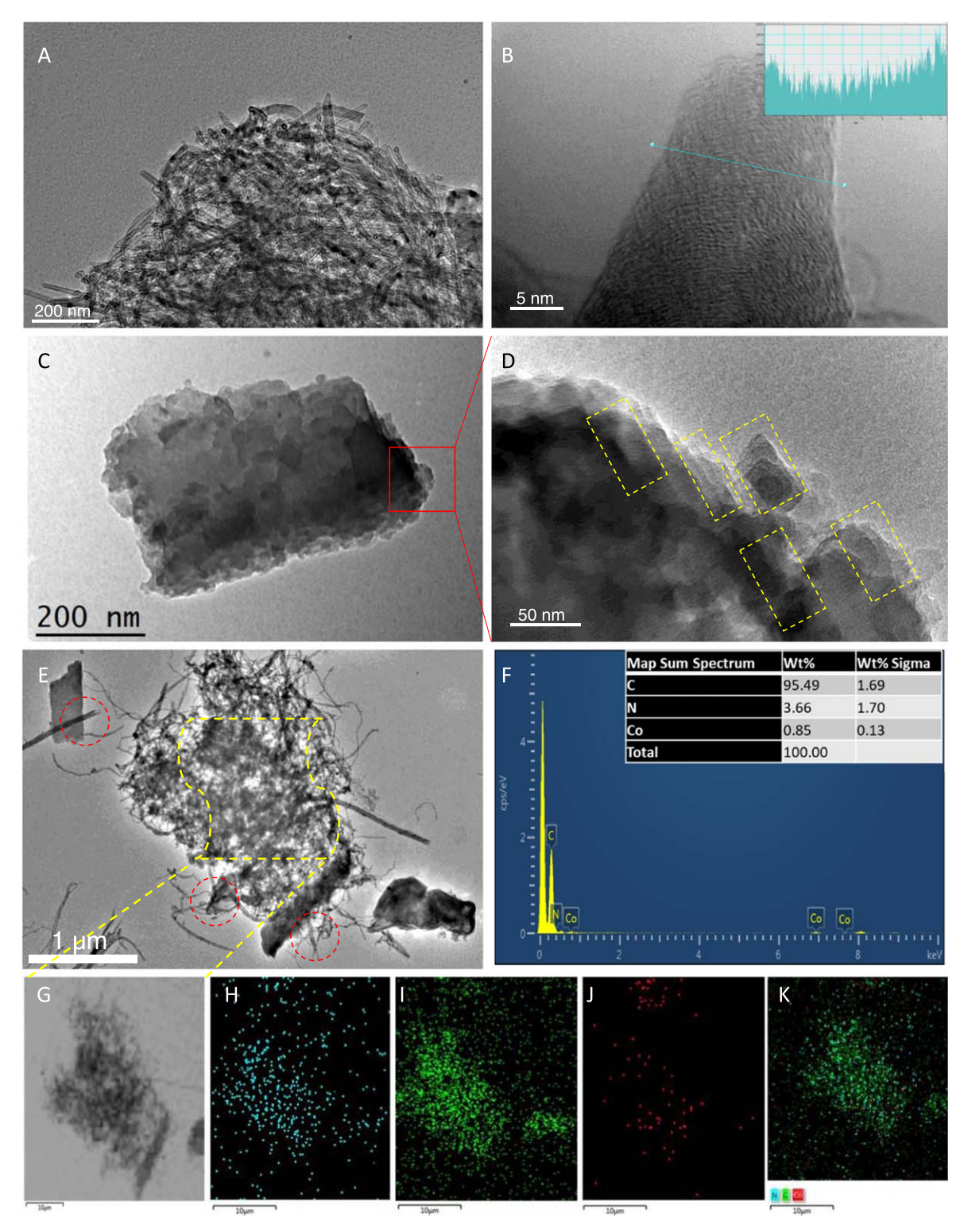


Figure 2. TEM images of (a)–(b) MWCNTs, (c)–(d) CoPc, and (e) CoPc/CNTs, (f) EDX pattern of CoPc/MWCNTs, (g)–(k) STEM-EDX mapping of CoPc/MWCNTs composites.

peaks appear but with stronger current in the applied potential range (0.5--1.2~V) in Fig. 3d. This phenomenon indicates that CNTs have no selectivity toward nitrite oxidation, cannot be used for an electrochemical nitrite sensor alone without other functional parts. 28 In addition, the stronger current behavior in Figs. 3a, 3b, 3d both confirm that MWCNTs are desired as conductive support for CoPc performing as an electrochemical sensor toward nitrite.

To gain acquaintance with the mechanism of the nitrite oxidation taking place at CoPc/MWCNTs electrode, CV at different scan rates in 0.1 M PBS (pH 7.0) with 0.1 M nitrite was performed, respectively (Fig. 4). The peak current of nitrite oxidation consistently increases with the square root of scan rate ($v^{1/2}$) shown in the inset of Fig. 4a by the fit equation as i_p (A) = 1.624 × 10⁻⁴ + 7.101 × 10⁻⁶ $v^{1/2}$ (R² = 0.9898). In addition, this linear dependence of the

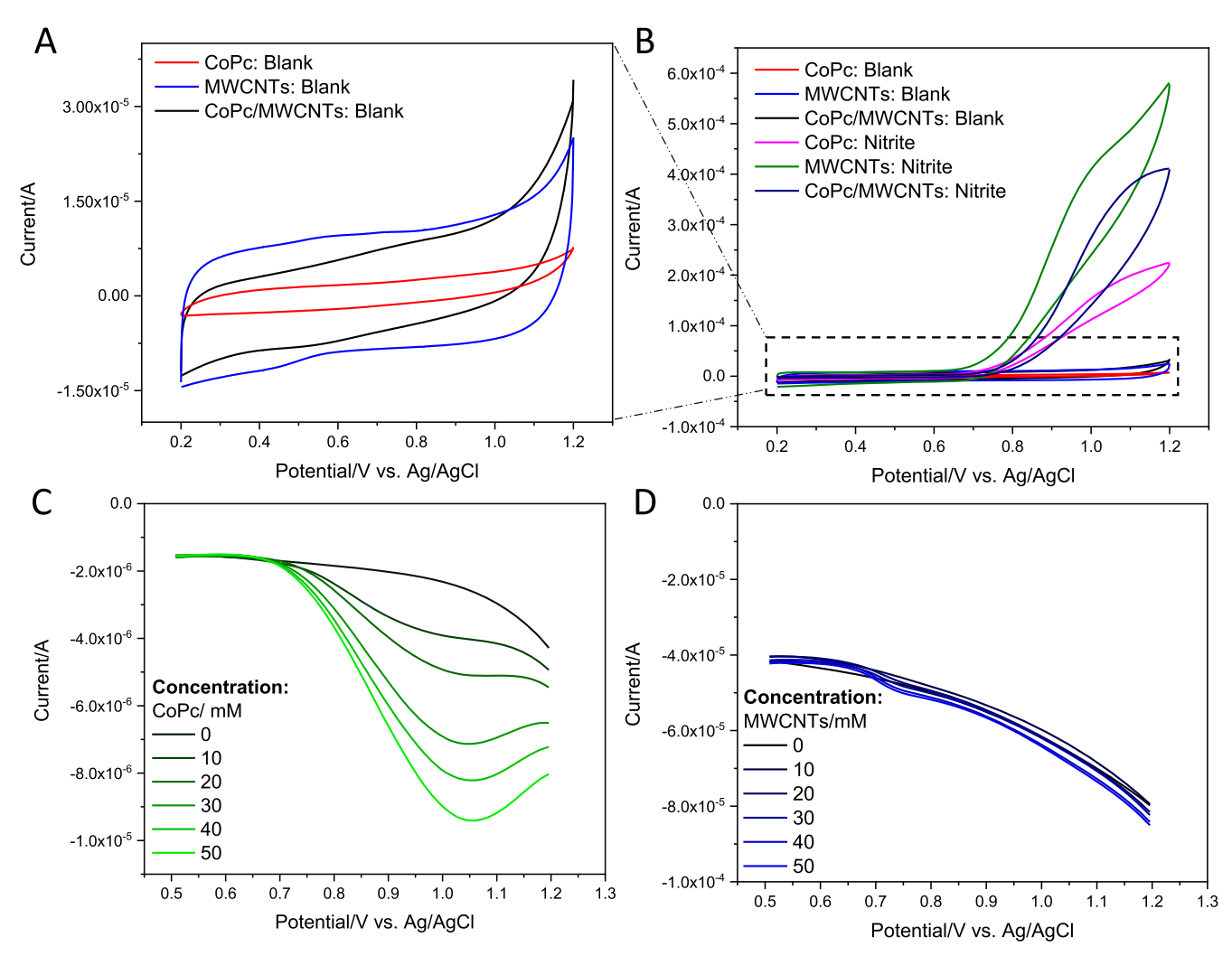


Figure 3. Cyclic voltammograms on the modified electrodes (CoPc, CNT and CoPc/CNT) in PBS (0.1 M, pH 7.0) without nitrite (a), with 0.1 M nitrite (b), scan rate: 50 mV s⁻¹. Differential pulse voltammograms of the modified electrodes (c) CoPc, (d) MWCNTs with different nitrite concentration from 0 to 5 mM in 0.1 M PBS (pH 7.0). DPV parameters: amplitude, 0.05 V; pulse width, 0.2 s; sampling width, 0.067 s; pulse period, 0.5 s.

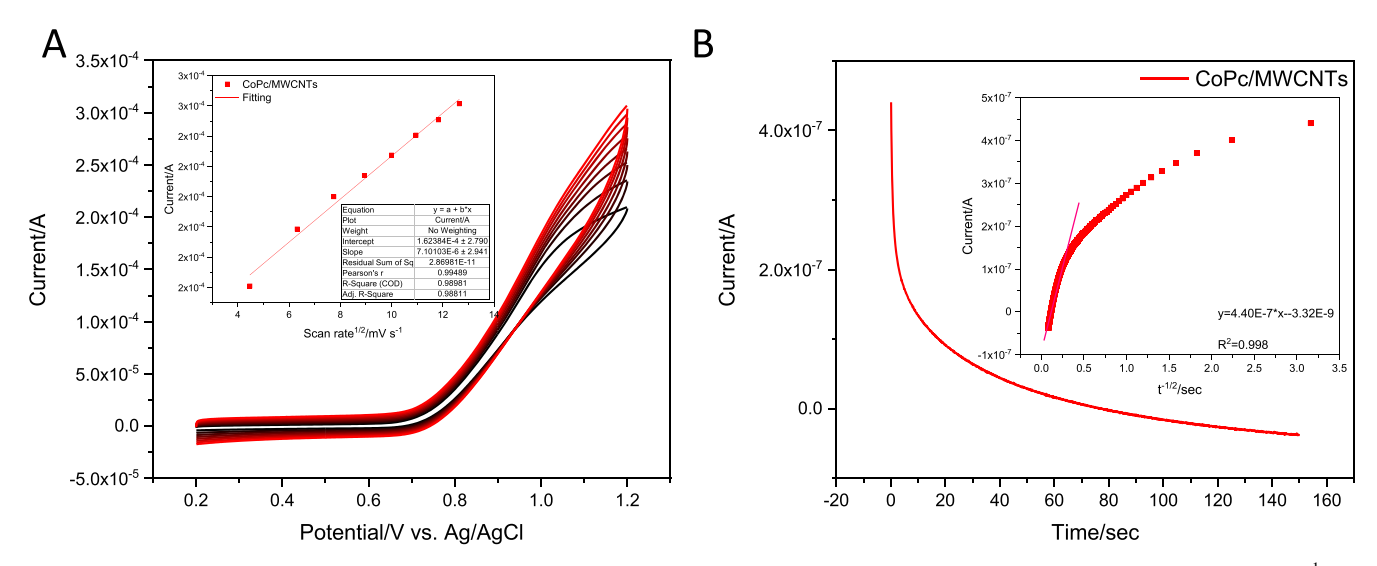


Figure 4. (a) Cyclic voltammograms of 0.1 M nitrite on CoPc/MWCNTs in 0.1 M PBS (pH 7.0) at different scan rates (from 20 (black) to 200 mV s⁻¹ (red)), inset: the plot of peak current vs. square root of scan rates. Amperometric i-t response of (b) CoPc/MWCNTs in 0.1 M PBS (pH 7.0) with 0.5 mM of nitrite solution at an applied potential of 0.9 V, inset: the plot of i vs t^{-1/2} derived from the amperometric i-t curve, respectively.

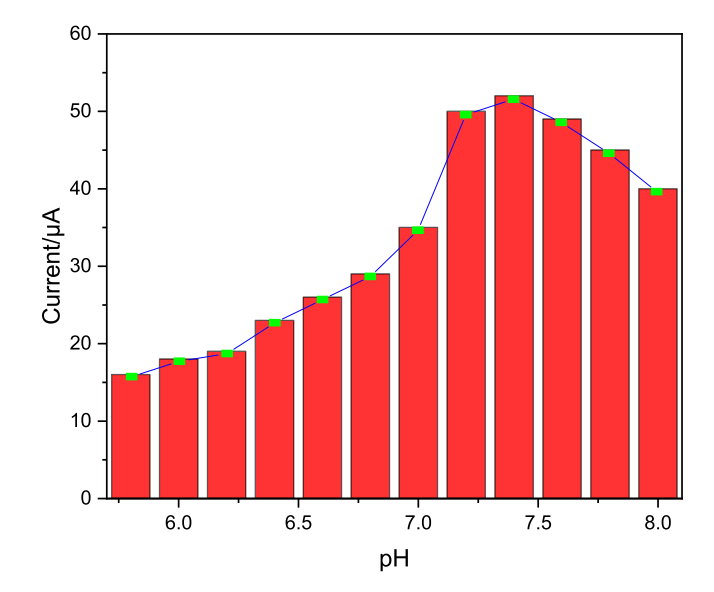


Figure 5. Current responses of CoPc/MWCNTs electrode with different pH values in PBS with 0.1 mM nitrite with a scan rate of 50 mV s^{-1} .

peak currents on the square root of scan rates as well as a near zero intercept indicates that the mechanism of nitrite oxidation on the surface of CoPc/MWCNTs modified electrode is under diffusion controlled. Similarly, amperometric *i-t* response was used to confirm the mechanism. Figure 4b depicts the amperometric *i-t* response of CoPc/MWCNTs modified electrode in 0.5 mM of nitrite under an applied voltage of 0.9 V. It is further verify that the oxidation of nitrite on the CoPc/MWCNTs electrode is a typical diffusion-controlled process, as presents in the inset of Fig. 4b. Noteworthy, the nitrite oxidation is a second-order homogeneous disporportionation process and the mechanism of the oxidation can be conveyed as: Eq. 1:^{2,29}

$$NO_2^- + H_2O \rightarrow NO_3^- + 2e^- + 2H^+$$
 [1]

The pH value in the electrolyte is a non-negligible parameter for nitrite oxidation. To assess the effect of pH on the nitrite oxidation at CoPc/MWCNTs electrode, the work was performed through CV measurement in 0.1 M PBS with a series of pH values (5.8–8.0) and the consequent peak currents are plotted as a function of pH in

Fig. 5. It is remarked that the peak current achieved a maximum value at pH 7.4 and then levelled off during nitrite oxidation implying the involvement of protons in the process owing to the production of N_2O at low pH which results in the decrease of the peak current.^{2,30} However, nitrite oxidation becomes more difficult as pH values arrives 8.0 due to the lack of protons. Additionally, the anodic peak potential shifts negatively with the increase of the pH. Therefore, considering the sensitive determination for nitrite pH 7.4 PBS was chose for the subsequent analytical experiments.

To further confirm the charge transfer properties, the CVs of CoPc, MWCNTs and CoPc/MWCNTs electrodes in 5.0 mM K₃Fe(CN)₆ solution containing 0.1 M KCl was also performed by the electrochemical method (Fig. 6a). As can be seen, a lower redox current with redox peaks separation was observed on CoPc modified electrode (green line in Fig. 6a) due to the redox of $[Fe(CN)_6]^{3-1}$ After modification, the anodic peak and cathodic peak (red line in Fig. 6a) of CoPc/MWCNTs@GCE are both enhanced ascribing to the enhanced electrical conductivity of MWCNTs modified electrode associated to CoPc@GCE, enhancing the electron transfer kinetics. The peak potentials of CoPc/MWCNTs@GCE almost not changes as the scan rate increased, and the separation potential from redox peaks is about 0.125 V (Fig. 6b). The ratio of I_{pq}/I_{pc} (oxidation peak current/reduction peak current) tends to 1. The number of electrons (n) engaged in this reaction was considered based on the linear relationship between the oxidation peak potential (E_n) and the logarithm of the scan rate ($\log \nu$), as shown in Eq. S1 (available online at stacks.iop.org/JES/167/046515/mmedia). The best linear fitting equation is $Ep = 0.043 \log \nu + 0.046$. n was calculated to be 2.15, suggesting a two-electron transfer process during nitrite oxidation, keeping consistent with the previous observation. This result further demonstrates the significance of the functionalization of CoPc with MWCNTs. 31,32

Electrochemical impedance spectroscopy (EIS) provides an insight to study the electron transfer process and impedance changes on the modified electrode surface. As displayed in Figs. 7a–7c, the Nyquist plots of CoPc@GCE, MWCNTs@GCE, and CoPc/MWCNTs@GCE in 5.0 mM $K_3 Fe(CN)_6$ containing 0.1 M KCl solution were recorded. The charge transfer resistance ($R_{\rm ct}$) of the modified electrode is calculated by the diameter of the semicircle in the Nyquist plot. Therefore, $R_{\rm ct}$ value for CoPc@GCE (Fig. 7a) was estimated to be 112.6 Ω , while this value decreased to 72.2 Ω on the CoPc/MWCNTs@GCE (Fig. 7c). This result indicates CoPc/MWCNTs electrode has lower electron transfer resistance than that of CoPc@GCE and MWCNTs@GCE owing to the conductive

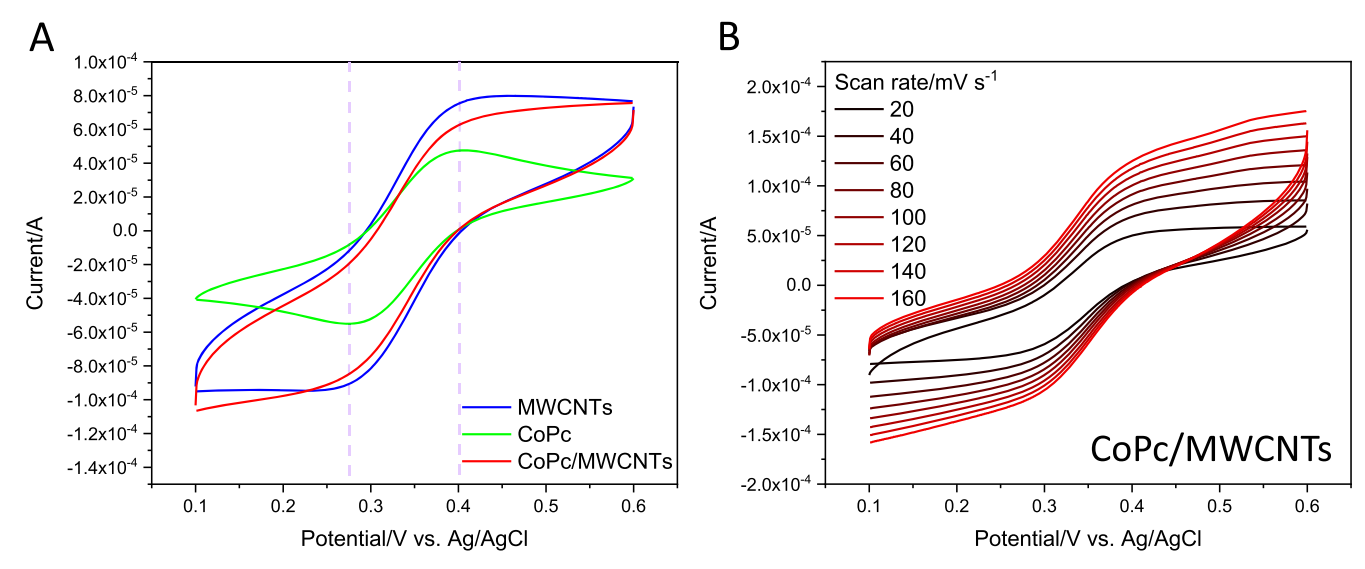


Figure 6. Cyclic voltammograms of the modified electrodes (CoPc: green line, MWCNTs: blue line, and CoPc/MWCNTs: red line) in the $5.0\,\text{mM}$ $K_3\text{Fe}(\text{CN})_6/0.1\,\text{M}$ KCl solution with (a) scan rate: $50\,\text{mV}\,\text{s}^{-1}$. (b) Cyclic voltammograms of CoPc/MWCNTs modified electrode in the $5.0\,\text{mM}$ $K_3\text{Fe}(\text{CN})_6/0.1\,\text{M}$ KCl solution with different scan rate from $20\,\text{to}\,160\,\text{mV}\,\text{s}^{-1}$.

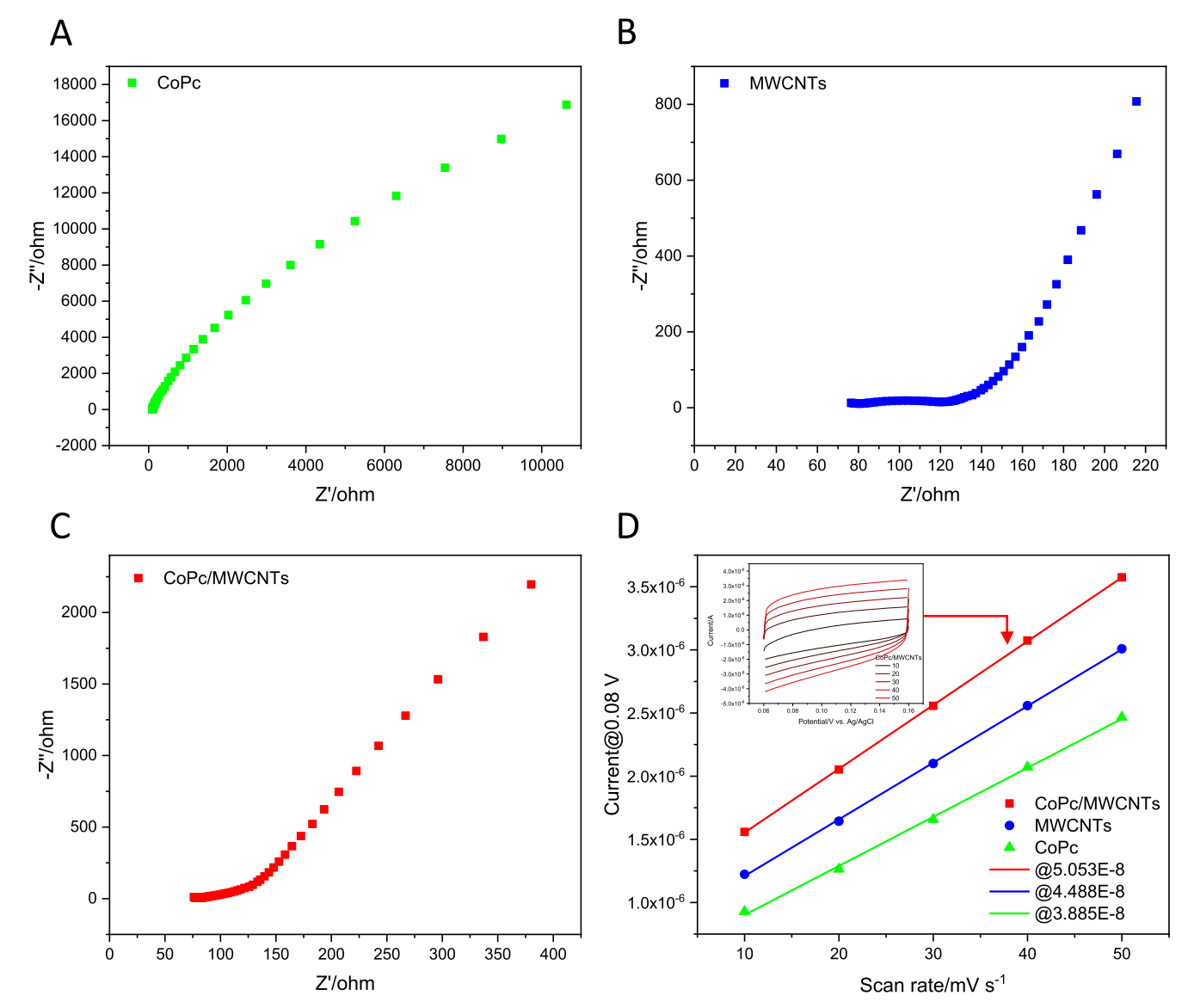


Figure 7. Nyquist plots (a) CoPc, (b) CNT, and (c) CoPc/CNT modified electrode in presence of $55.0 \text{ mM K}_3\text{Fe}(\text{CN})_6/0.1 \text{ M KCl}$ solution (d) plots of the averaged current density at 0.08 V against scan rates (CoPc: green line, CNT: blue line, and CoPc/CNT: red line). Inset: cyclic voltammograms of CoPc/CNT electrode in a narrow potential range of 0.06-0.16 V in 0.1 M PBS at different scan rates ($10-50 \text{ mV s}^{-1}$).

support of MWCNTs and amounts of electroactive species of CoPc, which can promote the facilitation of charge transfer between the redox probe and electrode surface by decreasing the electron transfer resistance.

Moreover, the double layer capacitance C_{dl} has been investigated to assess the active surface areas of CoPc, MWCNTs and CoPc/MWCNTs modified electrodes (Fig. 7d) by CV measurements in a narrow potential range (nonfaradaic process) with different scan rates. $^{33-36}$ After calculation, the specific surface area of CoPc/MWCNTs electrode is about $67.1\,\mathrm{cm^2}$ higher than MWCNTs (59.5 cm²) and CoPc (51.5 cm²), implying that the effective active sites of CoPc/MWCNTs for nitrite oxidation is higher than that of CoPc and MWCNTs. From EIS analysis and C_{dl} calculation, it is proved that CoPc/MWCNTs modified electrode could be a promising electrochemical platform for sensing.

Selectivity of CoPc/MWCNTs modified electrode.—To investigate the practical applications of the prepared sensor for nitrite detection, the dependence of the oxidation peak current on the concentration of nitrite was examined in 0.1 M PBS (pH 7.4). Figure 8a shows the DPV of nitrite with various concentrations at

the CoPc/MWCNTs@GCE with the nitrite concentration from 0.01 to 1050 mM. Several potentials are applied to compare the performance of the as-prepared sensor, as shown in Fig. 8b. Consequently, the slope of the function of concentration vs current (Fig. 8b and Table SI) under an applied potential of 0.972 V shows maximum value than other potentials (Fig. 8c). Therefore, the oxidation peak current increased linearly with the nitrite concentration from 0.01 to 1050 mM under 0.972 V, and the linear fitting equation for nitrite detection is $I_{pc}(mA) = -0.004c(mM) -7.59$ with a correlation coefficient of 0.99997 (Fig. 8d). Additionally, the lowest detection limit (LOD) is calculated to be 2.11 μ M, defined as three times the signal-to-noise ratio (S/N = 3). The results for different electrochemical sensors for nitrite determination are summarized in Table I. It is evident that CoPc/MWCNTs modified electrode has a wide linear response in a range from 10.0 μ M to 1050.0 mM with a detection limit of 2.11 μ M, which is lower than or comparable to those of other electrochemical sensors.

The stability of CoPc/MWCNTs@GCE was investigated through the continuous CV scan (Fig. 9a). The first CV cycle and the last 500th CV cycle are very near, implying that CoPc/MWCNTs@GCE can keep good stability in long time test. In addition, to test the

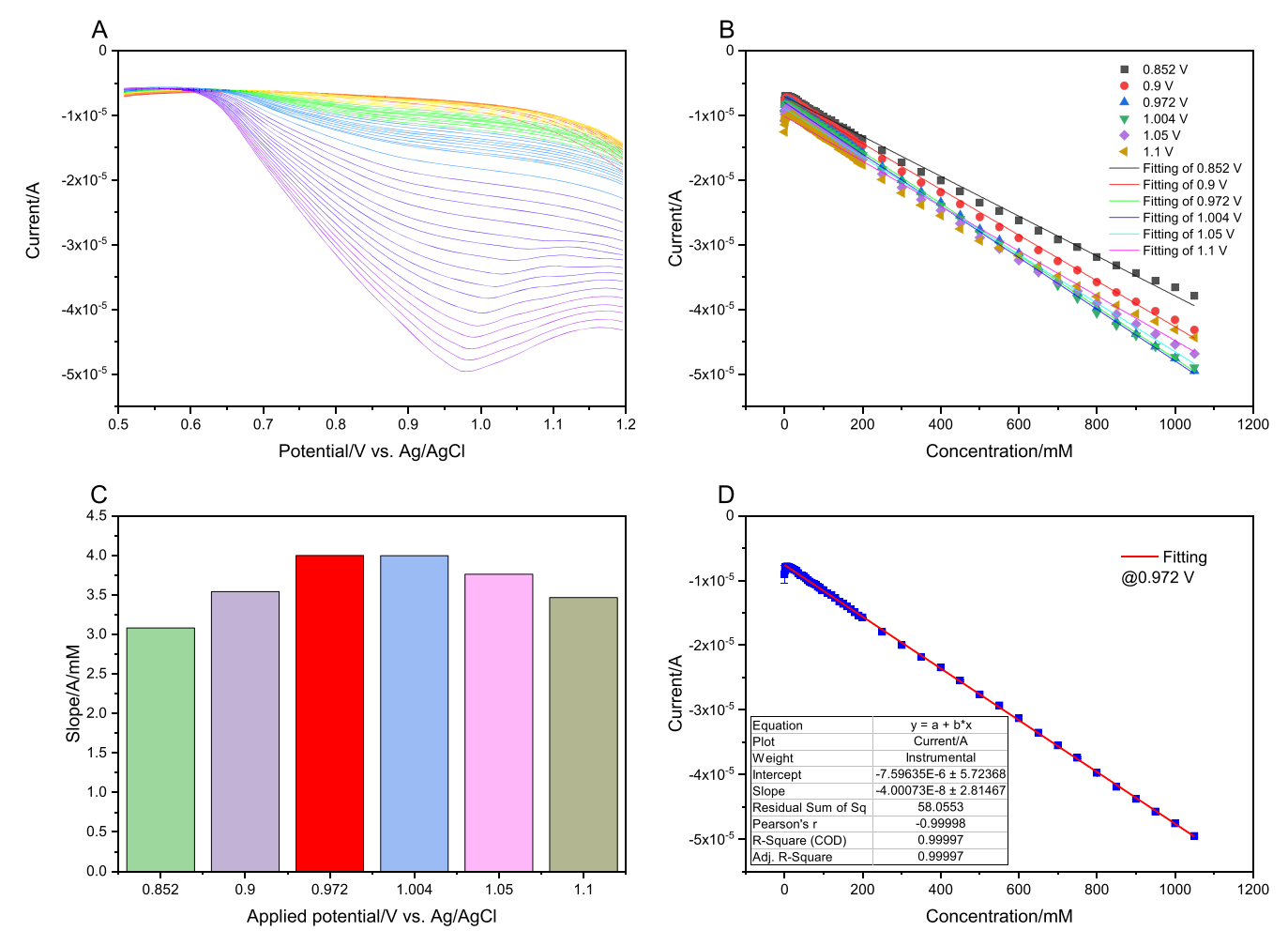


Figure 8. (a) Differential pulse voltammograms of CoPc/MWCNTs modified electrode toward nitrite detection with successive addition (0.01-1050 mM), (b) Optimized applied potential derived from Fig. 8a, (c) Performance (d) the plots of current vs concentration of NO_2^- from 0.01-1050 mM in PBS (pH = 7.4). DPV parameters: amplitude, 0.05 V; pulse width, 0.2 s; sampling width, 0.067 s; pulse period, 0.5 s.

selectivity of the CoPc/MWCNTs@GCE, the electrochemical response of 0.5 mM nitrite was evaluated in the several interferents (NaCl, Na₂SO₄, NaNO₃, CH₃COONa, and KCl) with 100-fold concentrations (50 mM) of the under the optimal conditions. However, glucose and ascorbic acid are regarded as potential interfering substances that usually coexist with nitrite in samples. As shown in Fig. 9b, there is an obvious current jump as nitrite injection in the first time, however, the current changes caused by

the addition of these interferents (NaCl, Na₂SO₄, NaNO₃, CH₃COONa, KCl, glucose, and ascorbic acid) were negligible, implying the highly selective sensing of nitrite with the CoPc/MWCNTs@GCE. It is worth mentioning that when nitrite was added into the stirring PBS solution, the CoPc/MWCNTs@GCE as a sensor responded rapidly and time is less than 7 s. The reproducibility of the CoPc/MWCNTs@GCE was investigated using a series of nitrite concentration (0.5, 5, 10, and 20 mM). The peak current

Table I. Comparison of CoPc/MWCNTs modified electrode with other sensors for nitrite detection employed glassy carbon electrode as the substrate.

Electrodes	Detection range/mM	$\mathrm{LOD}/\mu\mathrm{M}$	Technique	References
Cu/MWCNTs	0.005-1.26	1.8	Amperometry	37
Co ₃ O ₄ -DCS ^{a)}	0.0066-13.83	0.22	Amperometry	38
[TMPyPcCo/aCNTs] ₁₂ b)	0.005-30	2.6	Amperometry	17
f-ZnO@rFGO ^{c)}	0.01-8	33	Amperometry	39
Ag/Cu/MWNT	0.001-1	0.2	Amperometry	40
Pd/RGO	0.001-1	0.23	DPV	30
CoTMPyP/SrTa ₂ O ₇ ^{d)}	0.29-3.31	14	DPV	41
AuNPs/MoS2/GN ^e	0.005-5	1.0	Amperometry	32
CoPc/MWCNTs	0.01-1050	2.11	DPV	This work

a) disordered circular sheets. b) 2,9,16,23-tetra [4-(N-methyl)] pyridinyloxy phthalocyanine cobalt (II) sulfate and acid-treated multiwalled carbon nanotube c) flower-like zinc oxide (ZnO) and reduced functionalized graphene oxide (rFGO). d) 5, 10, 15, 20-tetrakis (N-methylpyridinium-4-yl) porphyrinato cobalt (III) on the $Bi_2SrTa_2O_9$

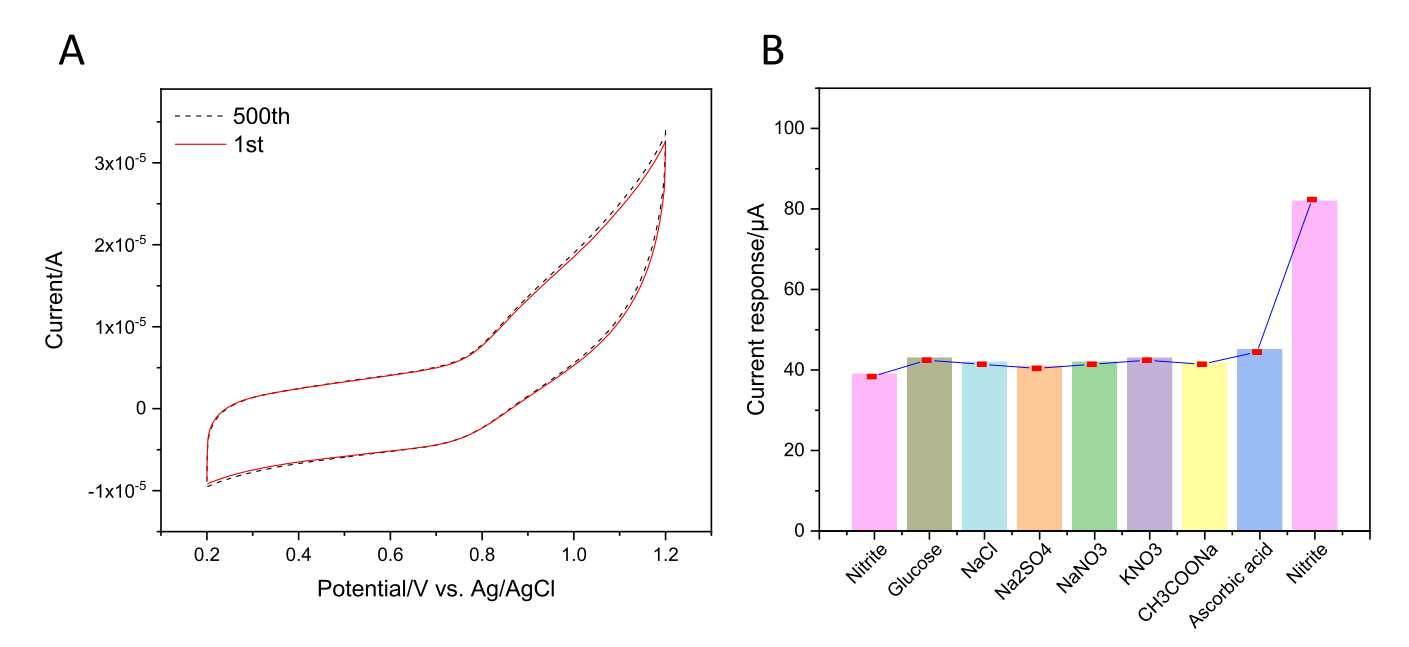


Figure 9. (a) Cyclic voltammograms of CoPc/MWCNTs modified electrode in 0.1 M PBS (pH = 7.4) solution with 0.1 mM nitrite obtained at the first cycle and the 500th cycle, (b) the signal enhancement of current in the presence of diverse kinds of interfering substance, respectively.

Table II. Determination of nitrite in 0.1 M PBS (with optimized conditions, n = 4).

Sample	Added/mM	Found/mM	Recovery/%	RSD/%
1	0.5	0.45	90	2.35
2	5	4.96	99.2	2.16
3	10	10.08	100.8	1.47
4	20	20.54	102.7	3.64

response of nitrite was determined using four different electrodes, which were produced under the same conditions. The relative standard deviation (n = 4, Table II) was calculated to be 3.64% and the recovery values of the samples are between 90.0% and 102.7%, indicating the as-prepared sensor was reproducible.

Conclusion

In summary, cobalt (II) phthalocyanine (CoPc) was immobilized on multiwalled carbon nanotubes (MWCNTs) and performed as modified electrode for urea determination. Various characterizations were applied, especially for TEM and STEM-EDX. The simple preparation of CoPc/MWCNTs makes is possible for the development of new electrode modified materials for nitrite detection. The CoPc/MWCNTs modified electrode exhibits wider linear range (0.01 to 1050 mM), low detection limit of 2.11 μ M (signal noise ratio is 3). Besides, the as-prepared electrochemical sensor presented good selectivity and satisfactory results in real sample application. The enhanced effectiveness attributes to the coupling effect of CoPc and MWCNTs, which could provide more exposed active sites and excellent conductivity.

Acknowledgments

This study was received research grants from NASA EpsCor (No. NNX16AQ98A), USDA-NIFA Hatch (No.SD00H618-16, SD00R680-19 NC1194), and NSF/EPSCoR (No. OIA-1849206, South Dakota 2D Materials for Biofilm Engineering, Science and Technology Center (2DBEST)). S. Lu also acknowledges the financial support from the China Scholarship Council (CSC).

ORCID

Shun Lu https://orcid.org/0000-0003-4287-0779

References

- 1. H. Y. Yin, Y. Wan, and L. Wang, J Nanosci Nanotechno, 19, 5279 (2019).
- 2. S. Lu, C. Yang, and M. Nie, J. Alloys Compd., 708, 780 (2017).
- X. Li, J. Ping, and Y. Ying, TrAC, Trends Anal. Chem., 113, 1 (2019).
- Z. Liu, V. S. Manikandan, and A. Chen, Current Opinion in Electrochemistry, 16,
- 5. K. Nithyayini, M. Harish, and K. Nagashree, *Electrochim. Acta*, 317, 701 (2019).
- Z. Fan, L. Sun, S. Wu, C. Liu, M. Wang, J. Xu, X. Zhang, and Z. Tong, J. Mater. Sci., 54, 10204 (2019).
- J. F. van Staden and T. A. van der Merwe, Microchim. Acta, 129, 33 (1998).
- 8. H. Chen, T. Yang, F. Liu, and W. Li, *Sensors Actuators B*, **286**, 401 (2019).
- 9. H. Bagheri, A. Hajian, M. Rezaei, and A. Shirzadmehr, J. Hazard. Mater., 324, 762 (2017)
- 10. E. F. S. Authority, EFSA Journal, 6, 689 (2008).
- 11. N. Adarsh, M. Shanmugasundaram, and D. Ramaiah, Anal. Chem., 85, 10008 (2013).
- 12. C. D. García, A. G. Crevillén, and A. Escarpa, Carbon-based Nanomaterials in Analytical Chemistry (Royal Society of Chemistry, London) (2018).
- 13. M. Ghanei-Motlagh and M. A. Taher, Biosens. Bioelectron., 109, 279 (2018).
- 14. Z. Lin, W. Xue, H. Chen, and J.-M. Lin, Anal. Chem., 83, 8245 (2011). 15. L. J. Gimbert and P. J. Worsfold, TrAC, Trends Anal. Chem., 26, 914 (2007).
- 16. M. C. Breadmore, A. I. Shallan, H. R. Rabanes, D. Gstoettenmayr, A. S. Abdul Keyon, A. Gaspar, M. Dawod, and J. P. Quirino, *Electrophoresis*, 34, 29 (2013).
- 17. J. Zhang, Z. Chen, H. Wu, F. Wu, C. He, B. Wang, Y. Wu, and Z. Ren, Journal of Materials Chemistry B, 4, 1310 (2016).
- 18. F. Bedioui and S. Griveau, Electroanalysis, 25, 587 (2013).
- 19. R. Chokkareddy, G. G. Redhi, and T. Karthick, Heliyon, 5, e01457 (2019).
- 20. Z. W. Peng, D. Yuan, Z. W. Jiang, and Y. F. Li, *Electrochim. Acta*, 238, 1 (2017).
- 21. K. M. Korfhage, K. Ravichandran, and R. P. Baldwin, Anal. Chem., 56, 1514 (1984).
- 22. M. Rangel Argote, E. Sánchez Guillén, A. G. Gutiérrez Porras, O. Serrano Torres, C. Richard, J. H. Zagal, F. Bedioui, S. Gutierrez Granados, and S. Griveau, Electroanalysis, 26, 507 (2014).
- F. Demir, H. Y. Yenilmez, A. Koca, and Z. A. Bayır, J. Electroanal. Chem., 832,
- 24. M. D. Brown and M. H. Schoenfisch, Electrochim. Acta, 273, 98 (2018).
- 25. S. Chaiyo, E. Mehmeti, W. Siangproh, T. L. Hoang, H. P. Nguyen, O. Chailapakul, and K. Kalcher, Biosens. Bioelectron., 102, 113 (2018).
- 26. S. Nantaphol, W. Jesadabundit, O. Chailapakul, and W. Siangproh, J. Electroanal. Chem., 832, 480 (2019).
- 27. Z. Zhao, J. Zhang, W. Wang, Y. Sun, P. Li, J. Hu, L. Chen, and W. Gong, Appl. Surf. Sci., 485, 274 (2019).
- 28. L. Jiang, R. Wang, X. Li, L. Jiang, and G. Lu, Electrochem. Commun., 7, 597 (2005)
- 29. R. Guidelli, F. Pergola, and G. Raspi, Anal. Chem., 44, 745 (1972).
- 30. L. Fu, S. Yu, L. Thompson, and A. Yu, RSC Adv., 5, 40111 (2015).
- 31. L. Lu, Sensors Actuators B, 281, 182 (2019).

- 32. Y. Han, R. Zhang, C. Dong, F. Cheng, and Y. Guo, Biosens. Bioelectron., 142, 111529 (2019).
- 33. S. Lu, M. Hummel, Z. Gu, Y. Gu, Z. Cen, L. Wei, Y. Zhou, C. Zhang, and C. Yang,

- S. Lu, M. Hummel, Z. Gu, Y. Gu, Z. Cen, L. Wei, Y. Zhou, C. Zhang, and C. Yang, Int J Hydrogen Energ, 44, 16144 (2019).
 S. Trasatti and O. Petrii, J. Electroanal. Chem., 327, 353 (1992).
 R. M. Penner and C. R. Martin, Anal. Chem., 59, 2625 (1987).
 B. S. Yeo and A. T. Bell, The Journal of Physical Chemistry C, 116, 8394 (2012).
- 37. D. Manoj, R. Saravanan, J. Santhanalakshmi, S. Agarwal, V. K. Gupta, and R. Boukherroub, *Sensors Actuators B*, **266**, 873 (2018).

 38. V. Sudha, S. A. Mohanty, and R. Thangamuthu, *New J. Chem.*, **42**, 11869 (2018).
- 39. A. Pandikumar, N. Yusoff, N. M. Huang, and H. N. Lim, *Microchim. Acta*, 182, 1113 (2015).
- Y. Zhang et al., Sensors Actuators B, 258, 1107 (2018).
 Z. Fan, Z. Ding, X. Zhang, S. Wu, M. Wang, and Z. Tong, Mater. Lett., 253, 281 (2019).